Calcium carbonate crystallization, agglomeration and form during continuous precipitation from solution

J. Phys. D: Appl. Phys. 24 (1991) 165–170. Printed in the UK

Calcium carbonate crystallization, agglomeration and form during continuous precipitation from solution

J Hostomský† and A G Jones

Department of Chemical and Biochemical Engineering, University College London, Torrington Place, London WC1E 7JE, UK

Received 11 June 1990, in final form 22 October 1990

Abstract. Experiments were carried out to study the precipitation of calcium carbonate resulting from the mixing of aqueous solutions of calcium nitrate and sodium carbonate in a continuous-flow crystallizer at 25 °C in the pH range 8.5 to 10.5, reagent concentration 0.025 to 0.2 mol/l and solution residence times of 5 to 20 min. The population balance model is used to estimate nucleation, growth and agglomeration rates. Under the conditions studied, agglomeration of individual, previously formed crystals largely determines particle size and at higher reagent concentrations results in a bimodal distribution. The crystal form depends on the concentration of reagents, pH and residence time.

1. Introduction

The crystal form of precipitated calcium carbonate at low supersaturation is largely determined by crystallization kinetics and has been intensively studied. Few kinetic studies of calcium carbonate precipitation, however, have been carried out at high supersaturations of reacting solutions [1–3]. Crystallization of $CaCO_3$ in this case is complicated by the formation of various polymorphs, namely amorphous calcium carbonate, vaterite and aragonite which are unstable with respect to thermodynamically stable calcite (but can be sufficiently stable within the timescale of an experiment). Furthermore, at higher supersaturations considerable agglomeration (i.e. intergrowth and cementation of individual, previously formed, aggregating particles of crystalline product) occurs which renders difficult conventional kinetic analysis based on the evaluation of the particle size distribution of the precipitate.

In most of the previous studies of $CaCO_3$ crystallization, the experimental conditions were chosen so as to avoid agglomeration of crystals. Therefore, little information is available on the role agglomeration plays in the mechanism of increasing particle size and in the determination of particle form. In the present work the continuous flow MSMPR (mixed suspension, mixed product removal) technique was adopted which enables—in comparison with a batch arrangement—a more precise definition of experimental conditions and easier subsequent analysis of the individual processes occurring in the reaction system [4]. The objective of this paper is to report a preliminary study of $CaCO_3$ crystallization and agglomeration in a continuous precipitation crystallizer and their effect in determining the structural characteristics of the crystalline product.

2. Theory

The crystal size distribution in a model MSMPR crystallizer is a result of simultaneous nucleation, growth and agglomeration of crystalline particles. Let the number of particles with a characteristic size in the range L to $L + \mathrm{d}L$ be $n(L)\,\mathrm{d}L$. It is assumed that the frequency of successful binary collisions between particles (by particles we mean both single crystals and previously formed agglomerates) of size L' to $L' + \mathrm{d}L'$ and L'' to $L'' + \mathrm{d}L''$ is equal to $\beta_0 n(L')n(L'')\,\mathrm{d}L'\,\mathrm{d}L''$. The number density $n(L)$ and the collision frequency factor β_0 are related to some convenient volumetric basis, e.g. unit volume of suspension.

In the MSMPR crystallizer in the steady state, the increase of particle number density brought about by particle growth and agglomeration is compensated by

† Permanent address: Institute of Inorganic Chemistry, Czechoslovak Academy of Sciences, Majakovského 24, Prague, Czechoslovakia.

0022-3727/91/020165 + 06 $03.50

withdrawal of the product from the crystallizer. The population balance can then be written as [5]

$$\beta_0 \frac{L^2}{2} \int_0^L \frac{n(L')n(L'')\,dL'}{L''^2} - \beta_0 n(L) \int_0^\infty n(L')\,dL' - G\frac{dn(L)}{dL} = \frac{n(L)}{\tau} \quad (1)$$

(here $L'^3 + L''^3 = L^3$) with the boundary condition

$$n(0) = B^0/G \quad (2)$$

where

G is the linear growth rate of particles (expressed as a rate of change of the characteristic particle dimension);

B^0 is the nucleation rate, i.e. the number of elementary particles formed per unit time per unit volume of suspension;

τ is the average residence time of suspension in the crystallizer, calculated as the ratio of the active volume of the crystallizer and the volumetric flow rate of suspension.

It follows from equation (1) that in this approach the collision frequency factor β_0 (which in more general formulations appears as a size-dependent kernel in the integrals in equation (1)) and the growth rate G are assumed to be independent of the particle size. Conversely, the values of these parameters evaluated from experimental data will represent certain averages over the size range involved. Further, no breakage or attrition terms are included in the model.

To our knowledge, an analytical solution of equation (1) is not available. However, considerable effort has been given in the literature to develop numerical solutions of the equations of this or similar type which appear in many problems concerning particulate processes [6–8]. Generally, the computational requirements are substantial. The efficiency of the numerical solution is important in the present study, since equation (1) has to be solved repeatedly within optimization procedures used in the evaluation of kinetic parameters from experimental data. In this work, a calculation scheme proposed by Hounslow and coworkers [9, 10] was adopted. Using this approach, the domain of particle sizes, $L_1 < L < L_{i\max}$, is divided according to a geometric progression with a quotient $2^{1/3}$, i.e. $L_i = L_{i-1}\,2^{1/3}$, into a relatively small number of classes, typically 20–40, in which the number and mass of particles are monitored. The number of particles in the ith size class (within the size interval L_i to L_{i+1}) is equal to N_i. In the steady state the balance equation for N_i analogous to equations (1) and (2) is

$$\left(\frac{dN_i}{dt}\right)_{agg} + \left(\frac{dN_i}{dt}\right)_{gro} + \left(\frac{dN_i}{dt}\right)_{nucl} = \frac{N_i}{\tau} \quad (3)$$

where subscripts agg, gro and nucl represent agglomeration, growth and nucleation.

Nucleation of particles affects only the first size class

$$\left(\frac{dN_i}{dt}\right)_{nucl} = \begin{cases} B^0 & \text{for } i = 1 \\ 0 & \text{for } i > 1. \end{cases} \quad (4)$$

For the agglomeration and growth term, Hounslow *et al* arrived at the expressions (written here for size-independent collision frequency factor β_0)

$$\frac{1}{\beta_0}\left(\frac{dN_i}{dt}\right)_{agg} = N_{i-1}\sum_{j=1}^{i-2} 2^{j-i+1} N_j + \tfrac{1}{2}N_{i-1}^2 - N_i\left(\sum_{j=1}^{i-1} 2^{j-i} N_j + \sum_{j=i}^{i_{\max}} N_j\right) \quad (5)$$

$$\left(\frac{dN_i}{dt}\right)_{gro} = \frac{G}{L_i}(aN_{i-1} + bN_i + cN_{i+1}) \quad (6)$$

where

$$a = -c = \frac{2r}{(1+r)(r^2-1)} \qquad b = \frac{2}{1+r}$$

and $r = 2^{1/3}$. In the present study, however, we have in the following way modified the growth term for the first size class to satisfy the condition of balance of the total number of crystals in the crystallizer. Thus, although the growth term in equation (6) contributes to the change of particle numbers in individual size classes, the total number of crystals in the system remains unchanged. Therefore, the sum of growth contributions in individual classes should be equal to zero, but summation of the growth terms according to (6) gives

$$\begin{aligned}\frac{1}{G}\sum_{i=1}^{i_{\max}}\left(\frac{dN_i}{dt}\right)_{gro} &= bN_1/L_1 + cN_2/L_1 \\ &\quad + aN_1/L_2 + bN_2/L_2 + cN_3/L_2 \\ &\quad + aN_2/L_3 + bN_3/L_3 + cN_4/L_3 \\ &= bN_1/L_1 + aN_1/L_2. \end{aligned} \quad (7)$$

The non-vanishing terms in the right-hand side of (7) represent in effect additional nucleation terms in the overall population balance (equation (3)). Therefore, in this work we use for the first size class the expression

$$\left(\frac{dN_1}{dt}\right)_{gro} = \frac{G}{L_1}[(b+cr)N_1 + cN_2] \quad (8)$$

which is constructed in such a way that the total number balance of particles is satisfied. After substitution from equations (4)–(8) into (3), a system of non-linear algebraic equations for N_i is obtained which approximates the original population balance (equation (1)).

3. Experimental procedure

The experimental set-up was essentially the same as described by Budz *et al* [11]. A small (300 cm^3) continuous flow crystallizer was fitted with a two-blade

Table 1. Summary of experimental conditions. C, calcite; ACC, amorphous calcium carbonate; $^+$, traces of calcite; V, vaterite (spherulitic); V_{hex}, vaterite (hexagonal platelets); (..), minor component.

Experiment	Reagent conc. (mol/l)	Residence time (min)	Production rate (g l^{-1} min^{-1})	Stirrer speed (RPM)	pH	Polymorph(s) formed
1	0.025	6.6	0.19	1800	8.5	C + (V)
2	0.025	5	0.25	1200	10.5	V^+
3	0.025	10	0.125	1200	10.5	V^+
4	0.05	5	0.50	1800	10.5	V
5	0.05	5	0.50	600	10.5	V
6	0.05	20	0.125	1200	10.5	V_{hex}
7	0.2	10	1.00	1200	8.5	C + (V) + (ACC)
8	0.2	10	1.00	1200	9.8	V + ACC
9	0.2	10	1.00	1200	10.5	V + ACC

stirrer, three vertical baffles, a pH electrode sensor, a periodically operated output valve and a thermostated jacket. The crystallizer was fed with equimolar solutions of $Ca(NO_3)_2$ and Na_2CO_3 which reacted to form a supersaturated solution of $CaCO_3$. The reagent solutions were prepared from distilled water and reagent grade salts. The flow rates were maintained to give suspension residence times in the range 5–20 min. Comparative experiments were carried out at different pH values and, therefore, a difference between the flow rates of both reagents was sometimes necessary. The stirrer speed was varied from 600 to 1800 RPM and the range of concentrations of inlet solutions was 0.025–0.2 mol/l. The solution concentrations were checked by volumetric analysis. All experimental runs were performed at 25 °C.

Particle size distribution in the samples of $CaCO_3$ suspensions withdrawn from the operating crystallizer was measured by a Malvern 3300 particle sizer which gives the relative frequency distribution on a volume basis. Measurements of particle size were carried out after achieving a steady state condition of the crystallizer operation (after six to ten residence times). The samples of 2 cm^3 volume were quickly transferred to the stirred measuring cell of the Malvern instrument. The sampling process took about two seconds. The dilution medium in the cell was obtained by filtering the suspension of $CaCO_3$ from the same experiment through a 0.30 μm membrane filter. Calcium carbonate precipitates were viewed by both optical microscopy and scanning electron microscopy and photographs were taken for a subsequent visual assessment.

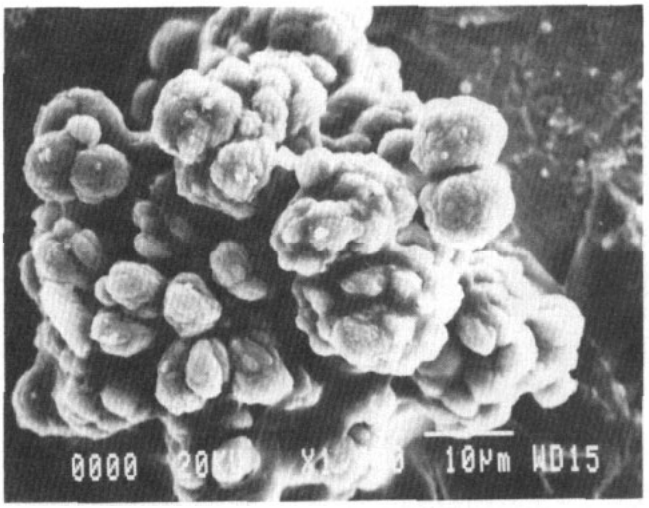

Figure 1. Agglomerates composed of spherical particles of vaterite (experiment 4).

4. Results and discussion

4.1. Structural aspects

Under the given experimental conditions (see table 1), agglomeration of individual, previously formed crystals rather than primary crystal growth was the dominant mechanism of increasing particle size. The morphology of agglomerates and individual crystals varied with precipitation conditions. Four basic different forms were observed (listed in table 1 and described below).

(i) At pH $\geq$ 9.5, mainly vaterite was precipitated, in the form of agglomerates of spherical particles (experiments 2 to 5, 8 and 9 in table 1; figure 1).

(ii) At the longest residence time (20 min at a pH of 10.5) the agglomerates were made up of thin hexagonal vaterite platelets (experiment 6; figure 2). This form of vaterite was observed earlier by Gibson *et al* [12] and by Meyer [13].

(iii) At higher reagent concentrations (experiments 7–9) a significant proportion of the product was formed by very fine gelatinous material which did not exhibit a discernible characteristic shape in the scanning electron microscope in the size range 80 to 100 nm. This phase we denote—following Ogino *et al* [14] and Brečevic and Nielsen [15]—amorphous calcium carbonate (ACC).

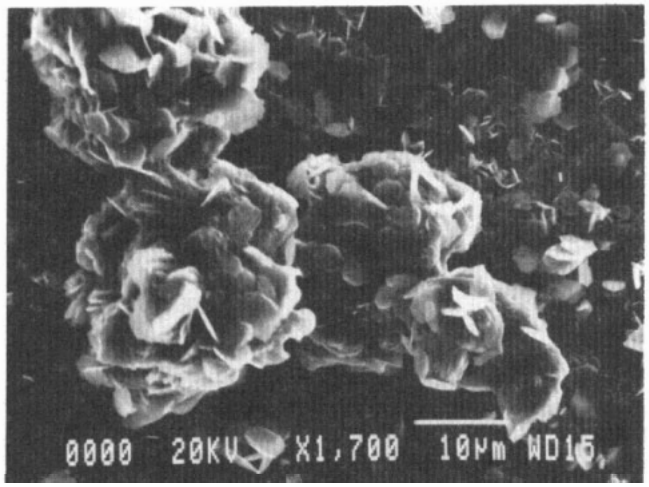

Figure 2. Agglomerates composed of hexagonal platelets of vaterite (experiment 6).

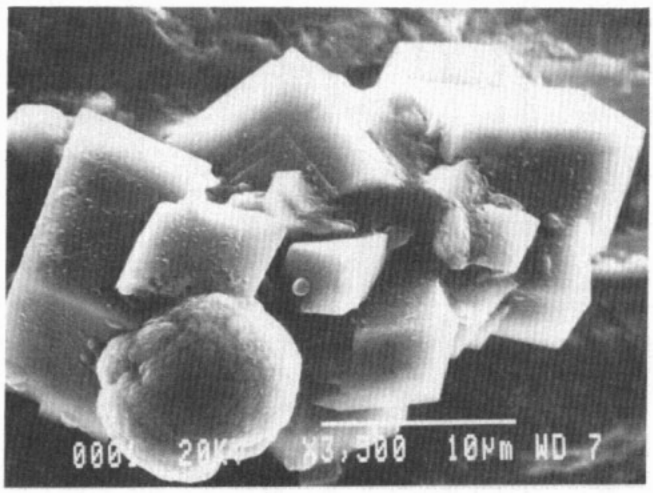

Figure 3. Agglomerate composed of calcite and vaterite (experiment 1).

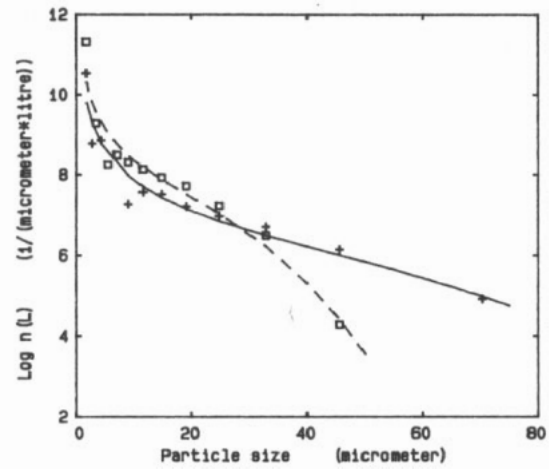

Figure 4. Effect of pH on population density. Experiment 7, pH 8.5, calcite: □, experimental data; – – –, model. Experiment 9, pH 10.5, vaterite: +, experimental data; ——, model.

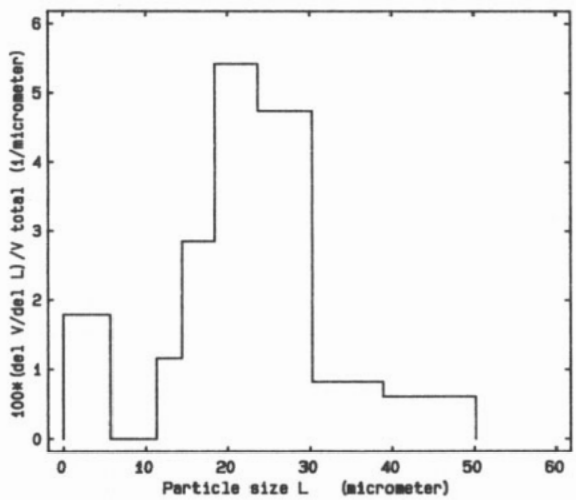

Figure 5. Particle volume distribution (experiment 1).

(iv) Agglomerates of calcite rhombs appeared at a lower alkalinity of suspension, i.e. a pH of 8.5 (experiments 1 and 7, figure 3). The shape of calcite agglomerates observed by scanning electron microscopy did not suggest twinning or growth from a single nuclei.

4.2. Population balance analysis

Distributions of particle sizes were plotted in the conventional semilogarithmic manner, $\log n(L)$ against L. All distributions exhibit a steep upward curvature in the region of smallest particles as shown in figure 4. They thus differ significantly from the well known ideal distribution of particle sizes in the product of the MSMPR crystallizer with size independent growth rates (i.e. straight lines in the semilogarithmic plots). The size distribution on the volume basis, which is the primary data yielded by the Malvern instrument, exhibits a bimodal shape with a secondary maximum in the region of smallest sizes (figure 5). To a lesser extent this feature is also manifested in the number distribution.

For a quantitative interpretation of the particle size distributions of agglomerated products from the continuous crystallizer, the kinetic parameters β_0, B^0 and G for individual experiments were estimated. The population balance equations were based on the formulation of Hounslow and co-workers [9–10] with the minimum size L_1 equal to 0.5 μm which corresponds approximately to the lower detection limit of the size analyser. The discrete equations were coded as a subroutine to the library modules [16] which iteratively solved the non-linear set of equations and minimized the objective function

$$S = \sum_{k=1}^{P} [\log n(L_k)_{\text{calc}} - \log n(L_k)_{\text{exp}}]^2. \qquad (9)$$

In equation (9), $n(L_k)_{\text{exp}}$ represents the number density

Table 2. Calculated values of parameters. N, set to zero in the two-parameter model.

Experiment	Collision frequency factor β ($\times 10^9$ l min^{-1})	Nucleation rate B^0 ($\times 10^{-12}$ l^{-1} min^{-1})	Growth rate G (μm min^{-1})	Apparent growth rate† G_{app} (μm min^{-1})	$(S/P)^{1/2}$
1	2.7	0.25	0.25	0.92	0.36
2	7.0	1.61	N	1.21	0.19
3	14.6	0.69	N	1.19	0.17
4	2.8	3.3	N	1.23	0.39
5	1.9	2.8	N	1.17	0.63
6	1.4	0.32	0.10	0.50	0.38
7	0.15	4.8	N	0.42	0.42
8	0.58	5.8	N	0.77	0.63
9	1.6	4.8	N	1.20	0.36

† Evaluated from the slope of the linear part of log $n(L)$ against L plot.

obtained from the volume percentage in the kth size class as measured by the Malvern instrument, $n(L_k)_{calc}$ is the number density calculated by means of population balance equations and P is the number of the size classes.

Firstly, each experimental size distribution was correlated by a full, three-parameter form of the discrete population balance (equation (3)), fitting the parameters β_0, B^0 and G. The three-parameter fits were successful only for size distributions obtained in precipitation of calcite and hexagonal platelets of vaterite at relatively mild conditions (experiments 1 and 6). For the remaining distributions, the fitting of the growth rate parameter G was found to be ill-conditioned, with the growth rate tending to zero and with unacceptably high confidence limits, indicating negligible contribution of the primary growth mechanism compared to agglomerative growth. The data are more successfully correlated by using only two parameters, i.e. with the collision frequency factor β_0 and nucleation rate B_0, and with the growth rate G in equations (3), (6) and (7) fixed to zero. The resulting kinetic parameter values are given in table 2 together with the values of average deviations $(S/P)^{1/2}$.

It follows from tables 1 and 2 that for comparable experiments the values of the collision frequency factor decrease with increasing mass production rate of crystals (calculated as half the ratio between the inlet reagent concentration and residence time). Thus, within the framework of the present size-independent agglomeration model, the relative efficiency of binary collisions decreases with increasing mass formation rate per unit crystallizer volume over the range studied. Significant lowering of a size-dependent agglomeration kernel with increasing production rates was also deduced, however, by Beckman and Farmer [17] from MSMPR experiments with a barium sulphate precipitation.

In experiments 4 and 5, where agglomerates of spherical vaterite particles were formed, the effect of the stirring rate at 600 and 1800 RPM was investigated. Figure 6 shows that whereas the size distribution in the region of smaller particles remains unaltered, at the higher stirring rate the higher sizes are more densely populated (in mass terms, 26% and 9% of particles are greater than 46 μm at 1800 and 600 RPM, respectively. The increase of agglomeration rate with increased stirring rate under the conditions of experiments 4 and 5 is reflected by a consequent increase in the collision frequency factor β_0 (table 2).

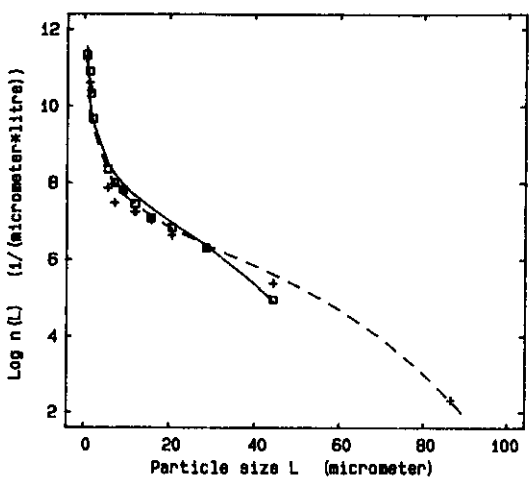

Figure 6. Effect of stirring rate on population density. Experiment 4, 1800 RPM: +, experimental data; – – –, model. Experiment 5, 600 RPM: □, experimental data; ——, model.

It is interesting to note that the crystal growth rates, determined by fitting the three-parameter model, are considerably lower than the (apparent) growth rates obtained by use of the conventional MSMPR analysis neglecting agglomeration [4]. In this method the apparent growth rate is determined from the slope A of the linear part in the log $n(L)$ against L plot, using the equation $G_{app} = 1/(2.303\,A\tau)$. Evidently, the apparent growth rates given in table 2 do not represent the true values of growth rates of primary particles which are discernible in figures 1 to 3. The crystal growth rates determined by three-parameter model fitting are roughly consistent with the primary particle sizes observed after a given residence time.

Experiments 7 to 9 (figure 4) dealing with the effect of pH, were carried out at the highest levels of reactant concentrations. It is apparent that in these experiments the collision frequency factor under the conditions of calcite formation is significantly lower than for vaterite formation and that the collision frequency factor increases strongly with increasing pH.

5. Conclusions

(i) During continuous precipitation of $CaCO_3$ the crystal form depends on the concentration of reactants, pH and crystallizer residence time.

(ii) At higher reagent concentrations crystal agglomeration determines particle size and results in a bimodal distribution.

(iii) The population balance model can be used to estimate growth, nucleation and agglomeration kinetic parameters simultaneously. Neglecting agglomeration in the analysis leads to overestimation of crystal growth rates.

Acknowledgment

The authors are indebted to Dr M J Hounslow, University of Cambridge, for helpful discussions on the discretized population balance analysis.

This work was supported by the UK SERC Specially Promoted Programme in Particulate Technology.

References

[1] Maruscak A, Baker C G J and Bergougnou M A 1971 *Can. J. Chem. Eng.* **49** 819

[2] Nakai T and Nakamaru H 1979 *Industrial Crystallization 78* eds E J de Jong and S J Jancic (Amsterdam: North-Holland) pp 75–9

[3] Söhnel O and Mullin J W 1982 *J. Cryst. Growth* **60** 239

[4] Randolph A D and Larson M A 1988 *Theory of Particulate Processes* 2nd edn (New York: Academic)

[5] Hulburt H M and Katz S 1964 *Chem. Eng. Sci.* **19** 555

[6] Hidy G M and Brock J R 1970 *The Dynamics of Aerocolloidal Systems* (New York: Pergamon)

[7] Sastry K V S and Gaschignard P 1981 *Ind. Eng. Chem. Fund.* **20** 355

[8] Gelbard F and Seinfeld J H 1978 *J. Comp. Phys.* **28** 357

[9] Hounslow M J, Ryall R L and Marshall V R 1988 *AIChE J.* **34** 1821

[10] Hounslow M J 1990 *AIChE J.* **36** 106

[11] Budz J, Jones A G and Mullin J W 1986 *J. Chem. Technol. Biotechnol.* **36** 153

[12] Gibson R E, Wyckoff R W G and Merwin H E 1925 *Am. J. Sci.* **10** 325

[13] Meyer H J 1965 *Z. Kristallogr.* **121** 220

[14] Ogino T, Suzuki T and Savada K 1987 *Geochim. Cosmochim. Acta* **51** 2757

[15] Brečevic L and Nielsen A E 1989 *J. Cryst. Growth* **98** 504

[16] *NAG Fortran Library* (Numerical Algorithms Group Ltd, Oxford, UK)

[17] Beckman J R and Farmer R W 1987 *AIChE Symp. Series* **253** 85